Applications of Mathematics

Yao-Chuang Han; Yu-Feng Nie; Zhan-Bin Yuan

Mathematical and numerical analysis of radiative heat transfer in semi-transparent media

*Applications of Mathematics*, Vol. 64 (2019), No. 1, 75–100

Persistent URL: http://dml.cz/dmlcz/147596

64 (2019) APPLICATIONS OF MATHEMATICS No. 1, 75–100

# MATHEMATICAL AND NUMERICAL ANALYSIS OF RADIATIVE HEAT TRANSFER IN SEMI-TRANSPARENT MEDIA

Yao-Chuang Han, Yu-Feng Nie, Zhan-Bin Yuan, Xian

Received October 22, 2017. Published online January 8, 2019.

*Abstract.* This paper is concerned with mathematical and numerical analysis of the system of radiative integral transfer equations. The existence and uniqueness of solution to the integral system is proved by establishing the boundedness of the radiative integral operators and proving the invertibility of the operator matrix associated with the system. A collocation-boundary element method is developed to discretize the differential-integral system. For the non-convex geometries, an element-subdivision algorithm is developed to handle the computation of the integrals containing the visibility factor. An efficient iterative algorithm is proposed to solve the nonlinear discrete system and its convergence is also established. Numerical experiment results are also presented to verify the effectiveness and accuracy of the proposed method and algorithm.

*Keywords*: radiative heat transfer; existence and uniqueness; collocation-boundary element method; shadow detection; iterative nonlinear solver

*MSC 2010*: 65M38, 45K05, 80A20, 47G10

## 1. Introduction

Radiative heat transfer is a major form of energy transport in many scientific and engineering fields such as astrophysics, nuclear reactors, reentry of space vehicles, and combustion in gas turbine combustion chambers. Interest in radiative heat transfer research has been very strong in several past decades due to its wide applications in those fields.

Mathematically, two types of models have been developed to describe the radiative heat transfer process. The first is the integro-differential radiative transfer equation (IDRTE) and the other is the radiative integral transfer equations (RITEs). The

This research was financially supported by the National Natural Science Foundation of China (Grant No. 11471262).

DOI: 10.21136/AM.2019.0276-17 

IDRTE model has been comprehensively investigated both mathematically and numerically in the past decades (cf. [2], [16], [22]). Due to its strong nonlinearity, developing fast iterative algorithms is critical for computing its solutions (cf. [1] and the references therein). Moreover, in the IDRTE model, the thermal radiation depends not only on the space and time variables but also on the angular variable which lives in a very high dimension space. This high dimensionality makes its approximation a very challenging task. On the other hand, the RITEs model is obtained by integrating the IDRTE model in the angular variable over all possible angles. As a result, the RITEs model is defined only in the space-time domain and it is angle-free. This technique eliminates the high dimension difficulty at a cost of dealing with integral operators with singular kernels and with linear and nonlinear systems of dense matrices.

Formulations and numerical simulation for RITEs have been carried out by several researchers. Crosbie [11], [12] derived a multi-dimensional RITEs model in bounded rectangular domain. Thynell [26] formulated a RITEs model in bounded two-dimensional cylindrical, absorbing, emitting, and linear-anisotropically scattering media. A set of integral equations for thermal radiative transmission in anisotropic scattering media was formulated in [25] and a product-integration teachnique was also used to discretize the model. Based on the alternative formulation of [25], Sun [24] developed a modified boundary element method for the thermal radiation problems. Li et al. [20] adopted the Galerkin boundary element method to discretize the thermal radiation problem without scattering. Altac [3], [4] used a singularity removal method to calculate the surface and volume integrals from the RITEs model.

In contrast to the situation for numerical simulation, very little attention has been paid to mathematical analysis for the RITEs model. To the best of our knowledge, the theoretical investigation for the RITEs model is mainly confined to the radiosity equation, which is the simplest case of the RITEs model. The radiosity equation has been extensively studied in [5], [6], [15], [23] and a collocation method for approximating the equation was proposed and analyzed in [5], where the unique solvability of the radiosity equation was proved by establishing some useful properties of the radiosity integral operator. We also refer the reader to [6] for a detailed discussion about numerical integrations required for the implementation of the proposed collocation method and to [15] for a regularity analysis of the solution of the radiosity equation on polyhedral surfaces. In [23], the authors presented a convergence and error analysis of the Galerkin boundary element method for the radiosity equation in both convex and non-convex domains. In addition, the coupling of heat radiation with other heat transfer mechanisms was studied in [19], [27]. The existence of a weak solution to the heat equation on a bounded non-convex domain with the Stefan-Boltzmann radiation boundary condition was proved by Laitinen in [19]

and some theoretical results for the coupled conduction-radiation heat transfer in semitransparent materials were obtained later in [27]. However, it seems that the mathematical analysis for the RITEs model in scattering media has not been investigated in the literature, such an analysis is important for understanding more complicate coupled energy transfer models. Filling this void is one of primary goals of this paper.

Moreover, for bounded non-convex domains, the detection of the shadow zone significantly affects the accuracy of the final results, and the detection simulation is very time-consuming. As a result, it became a bottleneck for the heat radiation simulation. Extensive research on this topic has been done in the past decades. We refer the reader to two monographs [10], [30] for a detailed exposition on the topic and to [14] for a summary and comparison of existing algorithms used in the heat radiation computation. In [8], the authors considered a two-dimensional problem with the subdivision of the current element based on the visibility of the all Gaussian nodes in the element. But the discrete distribution of Gaussian nodes contributes an additional (but unnecessary) error in this step. The algorithm proposed in [20] is based on the Galerkin boundary element method. It is well-known [7] that the Galerkin method requires the computation of surface and volume double integrations. To calculate the entries of the stiffness matrices, expensive integrations in four, five or six dimensions must be computed using the standard zoning method. To overcome this difficulty, in this paper we propose an efficient algorithm based on the idea of [8]. Moreover, in order to improve the accuracy of the computation, we introduce an element-subdivision technique to handle the visibility factor in the integral operators.

The remainder of this paper is organized as follows. In Section 2, we first present the formulation and physical background of the RITEs model. We then prove some properties for four radiative integral operators associated with the model. Section 3 is devoted to showing the existence and uniqueness theorem for the RITEs model. This is done by establishing the invertibility of the operator matrix associated with the model. In Section 4, we propose an iteration algorithm to be used as a nonlinear solver for solving the discretized nonlinear algebraic system, and prove its convergence by exploiting the properties of the radiative integral operators. In Section 5, we formulate a collocation-boundary element method to discretize the RITEs model. We also propose a new high-precision visibility algorithm to handle the computation of the integrals containing the visibility factor. In Section 6, we present some numerical experiment results to verify the effectiveness and accuracy of the proposed method and algorithms. Finally, the paper is completed with a few concluding remarks in Section 7.

## 2. Operator equation formulation for the RITEs model

We consider radiation transport in the bounded domain $V \subset \mathbb{R}^3$ with boundary $S$. The boundary is assumed to be diffuse and gray, which means that the emissivity and absorptivity of the surface are independent of the direction and wavelength of the radiation. In addition, we assume that the medium in the domain is homogeneous and isotropic.

Under the above assumptions, the RITEs model in an absorbing, emitting, and scattering medium can be written as follows (cf. [3]):

$$
\begin{aligned}
(2.1)\qquad & q(\mathbf{p}) + \varepsilon E_b(\mathbf{p}) \\
&= \varepsilon \int_S \Big( E_b(\mathbf{r}) + \frac{1-\varepsilon}{\varepsilon} q(\mathbf{r}) \Big) \exp(-\beta|\mathbf{p}-\mathbf{r}|) \frac{\cos\phi_p \cos\phi_r}{\pi|\mathbf{p}-\mathbf{r}|^2} \chi(\mathbf{p},\mathbf{r})\, \mathrm{d}S(\mathbf{r}) \\
&\quad + \varepsilon\sigma_a \int_V I_b(\mathbf{r}) \exp(-\beta|\mathbf{p}-\mathbf{r}|) \frac{\cos\phi_p}{|\mathbf{p}-\mathbf{r}|^2} \chi(\mathbf{p},\mathbf{r})\, \mathrm{d}V(\mathbf{r}) \\
&\quad + \frac{\varepsilon\sigma_s}{4\pi} \int_V G(\mathbf{r}) \exp(-\beta|\mathbf{p}-\mathbf{r}|) \frac{\cos\phi_p}{|\mathbf{p}-\mathbf{r}|^2} \chi(\mathbf{p},\mathbf{r})\, \mathrm{d}V(\mathbf{r}), \quad \mathbf{p} \in S, \\
(2.2)\qquad & G(\mathbf{p}) = \int_S \frac{1}{\pi} \Big( E_b(\mathbf{r}) + \frac{1-\varepsilon}{\varepsilon} q(\mathbf{r}) \Big) \exp(-\beta|\mathbf{p}-\mathbf{r}|) \frac{\cos\phi_r}{|\mathbf{p}-\mathbf{r}|^2} \chi(\mathbf{p},\mathbf{r})\, \mathrm{d}S(\mathbf{r}) \\
&\quad + \sigma_a \int_V I_b(\mathbf{r}) \exp(-\beta|\mathbf{p}-\mathbf{r}|) \frac{1}{|\mathbf{p}-\mathbf{r}|^2} \chi(\mathbf{p},\mathbf{r})\, \mathrm{d}V(\mathbf{r}) \\
&\quad + \frac{\sigma_s}{4\pi} \int_V G(\mathbf{r}) \exp(-\beta|\mathbf{p}-\mathbf{r}|) \frac{1}{|\mathbf{p}-\mathbf{r}|^2} \chi(\mathbf{p},\mathbf{r})\, \mathrm{d}V(\mathbf{r}), \quad \mathbf{p} \in V,
\end{aligned}
$$

where $q(\mathbf{p})$, $E_b(\mathbf{p})$, $I_b(\mathbf{p})$, $G(\mathbf{p})$ denote the radiative flux, blockbody emissive power, blockbody intensity of radiation and the incident energy at $\mathbf{p}$, respectively. The quantity $\varepsilon$ represents the emissivity of the boundary. The functions $\sigma_a$, $\sigma_s$, $\beta$ are the absorptivity, scattering coefficient, extinction coefficient with $\beta = \sigma_a + \sigma_s$. The symbol $\phi$ stands for the angle between the direction of the incoming ray and the outward normal direction of the boundary.

The Boolean function $\chi$ in equations (2.1)–(2.2), named the shadow zone function, is defined as

$$
\chi(\mathbf{p},\mathbf{r}) = \begin{cases} 1 & \text{if } \mathbf{r} \text{ can be seen by } \mathbf{p}, \\ 0 & \text{otherwise.} \end{cases}
$$

Here the statement "$\mathbf{r}$ can be seen by $\mathbf{p}$" means that there is no opaque material between $\mathbf{r}$ and $\mathbf{p}$ (i.e., $\overline{\mathbf{rp}} \bigcap S = \emptyset$).

Blockbody emissive power can be computed from the Stefan-Boltzmann law

$$
E_b(\mathbf{p}) = \sigma T^4(\mathbf{p}), \quad I_b(\mathbf{p}) = \frac{\sigma T^4(\mathbf{p})}{\pi},
$$

where $\sigma$ denotes the Stefan-Boltzmann constant and $T(\mathbf{p})$ is the temperature at $\mathbf{p}$.

So, once the temperatures of both the medium and the bounding surface are known, equations (2.1)–(2.2) can be rewritten in operator form as

$$K\mathbf{u} = \mathbf{f}, \tag{2.3}$$

where

$$\begin{aligned}
K &= \begin{pmatrix} I - K_1 & -K_2 \\ -K_4 & I - K_3 \end{pmatrix}, \ \mathbf{u} = \begin{pmatrix} q \\ G \end{pmatrix}, \ \mathbf{f} = \begin{pmatrix} f_1 \\ f_2 \end{pmatrix}, \\
(K_1 q)(\mathbf{p}) &= \frac{(1-\varepsilon)}{\pi} \int_S \exp(-\beta|\mathbf{p}-\mathbf{r}|) \frac{\cos\phi_p \cos\phi_r}{|\mathbf{p}-\mathbf{r}|^2} \chi(\mathbf{p},\mathbf{r}) q(\mathbf{r})\, \mathrm{d}S(\mathbf{r}), \\
(K_2 G)(\mathbf{p}) &= \frac{\varepsilon\sigma_s}{4\pi} \int_V \exp(-\beta|\mathbf{p}-\mathbf{r}|) \frac{\cos\phi_p}{|\mathbf{p}-\mathbf{r}|^2} \chi(\mathbf{p},\mathbf{r}) G(\mathbf{r})\, \mathrm{d}V(\mathbf{r}), \\
(K_3 G)(\mathbf{p}) &= \frac{\sigma_s}{4\pi} \int_V \exp(-\beta|\mathbf{p}-\mathbf{r}|) \frac{1}{|\mathbf{p}-\mathbf{r}|^2} \chi(\mathbf{p},\mathbf{r}) G(\mathbf{r})\, \mathrm{d}V(\mathbf{r}), \\
(K_4 q)(\mathbf{p}) &= \frac{1-\varepsilon re}{\varepsilon\pi} \int_S \exp(-\beta|\mathbf{p}-\mathbf{r}|) \frac{\cos\phi_r}{|\mathbf{p}-\mathbf{r}|^2} \chi(\mathbf{p},\mathbf{r}) q(\mathbf{r})\, \mathrm{d}S(\mathbf{r}), \\
f_1(\mathbf{p}) &= \varepsilon \int_S E_b(\mathbf{r}) \exp(-\beta|\mathbf{p}-\mathbf{r}|) \frac{\cos\phi_p \cos\phi_r}{\pi|\mathbf{p}-\mathbf{r}|^2} \chi(\mathbf{p},\mathbf{r})\, \mathrm{d}S(\mathbf{r}) - \varepsilon E_b(\mathbf{p}), \\
&\quad + \varepsilon\sigma_a \int_V I_b(\mathbf{r}) \exp(-\beta|\mathbf{p}-\mathbf{r}|) \frac{\cos\phi_p}{|\mathbf{p}-\mathbf{r}|^2} \chi(\mathbf{p},\mathbf{r})\, \mathrm{d}V(\mathbf{r}), \\
f_2(\mathbf{p}) &= \int_S E_b(\mathbf{r}) \exp(-\beta|\mathbf{p}-\mathbf{r}|) \frac{\cos\phi_r}{\pi|\mathbf{p}-\mathbf{r}|^2} \chi(\mathbf{p},\mathbf{r})\, \mathrm{d}S(\mathbf{r}), \\
&\quad + \sigma_a \int_V I_b(\mathbf{r}) \exp(-\beta|\mathbf{p}-\mathbf{r}|) \frac{1}{|\mathbf{p}-\mathbf{r}|^2} \chi(\mathbf{p},\mathbf{r})\, \mathrm{d}V(\mathbf{r}),
\end{aligned}$$

and $I$ denotes the identity operator.

In the next section, the properties of the four radiative integral operators $K_1$, $K_2$, $K_3$, $K_4$ will be analyzed separately.

## 3. Mathematical analysis of the RITEs model

In the existing references, the theoretical research about RITEs is confined to the radiosity equation, which does not take into account the scattering effect. One of the purposes of this paper is to make some contributions to this point. The integral system (2.3) is a coupled Fredholm integral system of the second kind. As is said in [18]: "Existence and uniqueness of a solution to an operator equation can be equivalently expressed by the existence of the inverse operator." So one way to

establish the existence and uniqueness of solution to the system (2.3) is to prove the existence of the inverse operator of $K$. In the following, we prove the boundness of radiative integral operators $K_1$, $K_2$, $K_3$, $K_4$. Based on these properties, the existence of the inverse operator of $K$ is obvious.

In this paper, we first extend Lemma 2.1 in [5] to non-convex domains and prove the following lemma.

**Lemma 3.1.** *Suppose $V$ is a bounded domain of $\mathbb{R}^3$ and has a Lipschitz boundary $S$. Let $\mathbf{p} \in S$, and let $S$ be smooth in an open neighborhood of $\mathbf{p}$. Besides, $\mathbf{p}$ can see all other points in the closure $\overline{V}$. Then*

$$\int_S \frac{\cos\phi_p \cos\phi_r}{|\mathbf{p}-\mathbf{r}|^2}\,\mathrm{d}S(\mathbf{r}) = \pi. \tag{3.1}$$

P r o o f. Let $\delta$ be a sufficiently small number. Exclude a $\delta$-neighborhood of $\mathbf{p}$ from $V$ and denote the remaining set by $V'$:

$$V' = V \setminus \{\mathbf{r} \in V\colon\ |\mathbf{r}-\mathbf{p}| \leqslant \delta\}.$$

Let $S'$ denote the boundary of $V'$ and let $S_\delta$ denote the boundary of $V \setminus V'$. Then

$$\int_S \frac{\cos\phi_p \cos\phi_r}{|\mathbf{p}-\mathbf{r}|^2}\,\mathrm{d}S(\mathbf{r}) = \int_{S'} \frac{\cos\phi_p \cos\phi_r}{|\mathbf{p}-\mathbf{r}|^2}\,\mathrm{d}S(\mathbf{r}) + \int_{S_\delta} \frac{\cos\phi_p \cos\phi_r}{|\mathbf{p}-\mathbf{r}|^2}\,\mathrm{d}S(\mathbf{r}). \tag{3.2}$$

For a continuously differentiable vector function $\mathbf{v}(\mathbf{r})$ defined on $V'$, the divergence theorem reads

$$\int_{S'} \mathbf{v}(\mathbf{r}) \cdot \mathbf{n}_r\,\mathrm{d}S(\mathbf{r}) = -\int_{V'} \nabla \cdot \mathbf{v}(r)\,\mathrm{d}V(\mathbf{r}). \tag{3.3}$$

Let

$$\mathbf{v}(\mathbf{r}) = \frac{(\mathbf{p}-\mathbf{r}) \cdot \mathbf{n}_p}{|\mathbf{r}-\mathbf{p}|^4}(\mathbf{r}-\mathbf{p}), \tag{3.4}$$

then the following result is obvious:

$$\nabla \cdot \mathbf{v}(\mathbf{r}) = 0, \quad \mathbf{r} \in V'. \tag{3.5}$$

Making use of equations (3.3)–(3.5), the first integral on the right-hand side of equation (3.2) can be computed as follows:

$$\int_{S'} \frac{\cos\phi_p \cos\phi_r}{|\mathbf{p}-\mathbf{r}|^2}\,\mathrm{d}S(\mathbf{r}) = \int_{S'} \frac{[(\mathbf{p}-\mathbf{r}) \cdot \mathbf{n}_p][(\mathbf{r}-\mathbf{p}) \cdot \mathbf{n}_r]}{|\mathbf{p}-\mathbf{r}|^4}\,\mathrm{d}S(\mathbf{r}) = 0. \tag{3.6}$$

For the second integral on the right-hand side of (3.2), the integral domain $S_\delta$ can be decomposed into two parts

$$S_\delta = T_\delta \cup W_\delta,$$

where

$$T_\delta = \{\mathbf{r} \in S\colon\ |\mathbf{r}-\mathbf{p}| \leqslant \delta\}, \quad W_\delta = \{\mathbf{r} \in V\colon\ |\mathbf{r}-\mathbf{p}| = \delta\}.$$

Then we have

$$\int_{S_\delta} \frac{\cos\phi_p \cos\phi_r}{|\mathbf{p}-\mathbf{r}|^2}\,\mathrm{d}S(\mathbf{r}) = \int_{T_\delta} \frac{\cos\phi_p \cos\phi_r}{|\mathbf{p}-\mathbf{r}|^2}\,\mathrm{d}S(\mathbf{r}) + \int_{W_\delta} \frac{\cos\phi_p \cos\phi_r}{|\mathbf{p}-\mathbf{r}|^2}\,\mathrm{d}S(\mathbf{r}). \tag{3.7}$$

According to the assumption that $\mathbf{p}$ can see all other points in the closure $\overline{V}$, the following inequalities are valid:

$$0 \leqslant \phi_p, \phi_r \leqslant \frac{\pi}{2},$$

which imply the inequality

$$\frac{\cos\phi_p \cos\phi_r}{|\mathbf{p}-\mathbf{r}|^2} \geqslant 0.$$

Besides, from [12] we have

$$\frac{\cos\phi_p \cos\phi_r}{|\mathbf{p}-\mathbf{r}|^2} \leqslant c \quad \text{for } \mathbf{p}, \mathbf{r} \in S,\ \mathbf{p} \neq \mathbf{r},$$

where $c$ is independent of $\mathbf{p}$ and $\mathbf{r}$.

Then

$$0 \leqslant \int_{T_\delta} \frac{\cos\phi_p \cos\phi_r}{|\mathbf{p}-\mathbf{r}|^2}\,\mathrm{d}S(\mathbf{r}) \leqslant c\int_{T_\delta} 1\,\mathrm{d}S(\mathbf{r}) = \mathrm{O}(\delta^2).$$

For the first integral on the right-hand side of (3.7), one obtains

$$\lim_{\delta\to 0} \int_{T_\delta} \frac{\cos\phi_p \cos\phi_r}{|\mathbf{p}-\mathbf{r}|^2}\,\mathrm{d}S(\mathbf{r}) = 0. \tag{3.8}$$

For any $\mathbf{r} \in W_\delta$, we have

$$\mathbf{n}_r = \frac{\mathbf{r}-\mathbf{p}}{|\mathbf{r}-\mathbf{p}|}, \quad \mathbf{n}_r \cdot \frac{\mathbf{r}-\mathbf{p}}{|\mathbf{r}-\mathbf{p}|} = 1.$$

Consequently,

$$\begin{aligned}
&\int_{W_\delta} \frac{\cos\phi_p \cos\phi_r}{|\mathbf{p}-\mathbf{r}|^2}\,\mathrm{d}S(\mathbf{r}) \\
&\quad = \int_{W_\delta} \frac{[(\mathbf{p}-\mathbf{r})\cdot\mathbf{n}_p][(\mathbf{r}-\mathbf{p})\cdot\mathbf{n}_r]}{|\mathbf{p}-\mathbf{r}|^4}\,\mathrm{d}S(\mathbf{r}) = \int_{W_\delta} \frac{(\mathbf{p}-\mathbf{r})\cdot\mathbf{n}_p}{|\mathbf{p}-\mathbf{r}|^3}\,\mathrm{d}S(\mathbf{r}) \\
&\quad = \frac{1}{\delta^3}\int_{W_\delta} (\mathbf{p}-\mathbf{r})\cdot\mathbf{n}_p\,\mathrm{d}S(r) = \frac{1}{\delta^3}\int_0^{2\pi}\int_0^{\pi/2} \delta\cos\varphi\delta^2\sin\varphi\,\mathrm{d}\varphi\,\mathrm{d}\theta.
\end{aligned}$$

By means of a simple calculation to the above last integral, the following result holds:

$$\int_{W_\delta} \frac{\cos\phi_p \cos\phi_r}{|\mathbf{p}-\mathbf{r}|^2}\,\mathrm{d}S(\mathbf{r}) = \pi. \tag{3.9}$$

Substituting equations (3.8) and (3.9) into equation (3.7), one obtains

$$\lim_{\delta\to 0}\int_{S_\delta} \frac{\cos\phi_p \cos\phi_r}{|\mathbf{p}-\mathbf{r}|^2}\,\mathrm{d}S(\mathbf{r}) = \pi. \tag{3.10}$$

Combining equations (3.6) and (3.10), equation (3.2) can be computed as

$$\int_{S} \frac{\cos\phi_p \cos\phi_r}{|\mathbf{p}-\mathbf{r}|^2}\,\mathrm{d}S(\mathbf{r}) = \pi.$$

This is the desired result and the proof is complete. □

**Lemma 3.2.** *Assume $S$ is a piecewise smooth surface of a bounded domain $V$ in $\mathbb{R}^3$. Let $\mathbf{p} \in S$ be a point at which $S$ is smooth. Then*

$$\int_S \exp(-\beta|\mathbf{p}-\mathbf{r}|)\frac{\cos\phi_p \cos\phi_r}{|\mathbf{p}-\mathbf{r}|^2}\chi(\mathbf{p},\mathbf{r})\,\mathrm{d}S(\mathbf{r}) \leqslant \pi, \tag{3.11}$$

$$\int_V \exp(-\beta|\mathbf{p}-\mathbf{r}|)\frac{\cos\phi_p}{|\mathbf{p}-\mathbf{r}|^2}\chi(\mathbf{p},\mathbf{r})\,\mathrm{d}V(\mathbf{r}) \leqslant \frac{\pi}{\beta}. \tag{3.12}$$

P r o o f. For any two points $\mathbf{p}$, $\mathbf{r}$, the following inequality holds:

$$\exp(-\beta|\mathbf{p}-\mathbf{r}|) \leqslant 1.$$

As a consequence, the following inequality is valid:

$$\int_S \exp(-\beta|\mathbf{p}-\mathbf{r}|)\frac{\cos\phi_p \cos\phi_r}{|\mathbf{p}-\mathbf{r}|^2}\chi(\mathbf{p},\mathbf{r})\,\mathrm{d}S(\mathbf{r}) \leqslant \int_S \frac{\cos\phi_p \cos\phi_r}{|\mathbf{p}-\mathbf{r}|^2}\chi(\mathbf{p},\mathbf{r})\,\mathrm{d}S(\mathbf{r}). \tag{3.13}$$

For any $\mathbf{p} \in S$, we can always find a bounded domain $V' \subset V$ with Lipschitz boundary $S'$ such that $\mathbf{p}$ can see all other points in the closure $\overline{V'}$. Then,

$$\int_S \frac{\cos\phi_p \cos\phi_r}{|\mathbf{p}-\mathbf{r}|^2}\chi(\mathbf{p},\mathbf{r})\,\mathrm{d}S(\mathbf{r}) = \int_{S'} \frac{\cos\phi_p \cos\phi_r}{|\mathbf{p}-\mathbf{r}|^2}\,\mathrm{d}S(\mathbf{r}). \tag{3.14}$$

Applying the result of Lemma 3.1 to the right-hand side of (3.14), we have

$$\int_{S'} \frac{\cos\phi_p \cos\phi_r}{|\mathbf{p}-\mathbf{r}|^2}\,\mathrm{d}S(\mathbf{r}) = \pi. \tag{3.15}$$

Based on equations (3.13)–(3.15), the inequality (3.11) holds.

As shown in [29],

$$\mathrm{d}L_{rp}(\mathbf{r}')\frac{\mathrm{d}S(\mathbf{r})\cos\phi_r}{|\mathbf{r}-\mathbf{p}|^2}=\frac{\mathrm{d}V(\mathbf{r}')}{|\mathbf{r}'-\mathbf{p}|^2}. \tag{3.16}$$

Adopting the above equality (3.16) and the idea of (3.14), we have

$$\begin{aligned}
&\int_V \exp\left(-\beta|\mathbf{p}-\mathbf{r}|\right)\frac{\cos\phi_p}{|\mathbf{p}-\mathbf{r}|^2}\chi(\mathbf{p},\mathbf{r})\,\mathrm{d}V(\mathbf{r})\\
&\quad=\int_S\left(\int_{L_{rp}}\exp(-\beta|\mathbf{p}-\mathbf{r}'|)\,\mathrm{d}L_{rp}(\mathbf{r}')\right)\frac{\cos\phi_p\cos\phi_r}{|\mathbf{p}-\mathbf{r}|^2}\chi(\mathbf{p},\mathbf{r})\,\mathrm{d}S(\mathbf{r})\\
&\quad=\int_{S'}\left(\int_{L_{rp}}\exp(-\beta|\mathbf{p}-\mathbf{r}'|)\,\mathrm{d}L_{rp}(\mathbf{r}')\right)\frac{\cos\phi_p\cos\phi_r}{|\mathbf{p}-\mathbf{r}|^2}\,\mathrm{d}S(\mathbf{r})\\
&\quad=\frac{1}{\beta}\int_{S'}(1-\exp(-\beta|\mathbf{p}-\mathbf{r}|))\frac{\cos\phi_p\cos\phi_r}{|\mathbf{p}-\mathbf{r}|^2}\,\mathrm{d}S(\mathbf{r})\leqslant\frac{1}{\beta}\int_{S'}\frac{\cos\phi_p\cos\phi_r}{|\mathbf{p}-\mathbf{r}|^2}\,\mathrm{d}S(\mathbf{r}).
\end{aligned}$$

With help of the above last inequality and (3.15), the following result can be obtained:

$$\int_V\exp(-\beta|\mathbf{p}-\mathbf{r}|)\frac{\cos\phi_p}{|\mathbf{p}-\mathbf{r}|^2}\chi(\mathbf{p},\mathbf{r})\,\mathrm{d}V(\mathbf{r})\leqslant\frac{\pi}{\beta}.$$

The proofs are complete. □

**Lemma 3.3.** *Assume $S$ is a piecewise smooth surface of a bounded domain $V$ in $\mathbb{R}^3$. Let $\mathbf{p}\in S$ be a point at which $S$ is smooth. Let $d$ denote the diameter of $V$. Then*

$$\int_V\exp(-\beta|\mathbf{p}-\mathbf{r}|)\frac{1}{|\mathbf{p}-\mathbf{r}|^2}\chi(\mathbf{p},\mathbf{r})\,\mathrm{d}V(\mathbf{r})\leqslant\frac{4\pi}{\beta}(1-\exp(-\beta d)), \tag{3.17}$$

$$\int_S\exp(-\beta|\mathbf{p}-\mathbf{r}|)\frac{\cos\phi_r}{|\mathbf{p}-\mathbf{r}|^2}\chi(\mathbf{p},\mathbf{r})\,\mathrm{d}S(\mathbf{r})\leqslant 4\pi. \tag{3.18}$$

P r o o f. For any point $\mathbf{p}\in V$, we can always find a bounded domain $V'\subset V$ with Lipschitz boundary $S'$, in which $\mathbf{p}$ can see all other points in the closure $\overline{V'}$. Then

$$\int_V\exp(-\beta|\mathbf{p}-\mathbf{r}|)\frac{1}{|\mathbf{p}-\mathbf{r}|^2}\chi(\mathbf{p},\mathbf{r})\,\mathrm{d}V(\mathbf{r})=\int_{V'}\exp(-\beta|\mathbf{p}-\mathbf{r}|)\frac{1}{|\mathbf{p}-\mathbf{r}|^2}\,\mathrm{d}V(\mathbf{r}). \tag{3.19}$$

Let $\delta$ be a sufficiently small value and denote by $B(\mathbf{p};\delta)$ a $\delta$-neighborhood of $\mathbf{p}$. Exclude $B(\mathbf{p};\delta)$ from $V'$, and denote the remaining domain by $V'_\delta$. Then we have

$$\begin{aligned}
&\int_{V'}\exp(-\beta|\mathbf{p}-\mathbf{r}|)\frac{1}{|\mathbf{p}-\mathbf{r}|^2}\,\mathrm{d}V(\mathbf{r})\\
&\quad=\int_{B(\mathbf{p};\delta)}\exp(-\beta|\mathbf{p}-\mathbf{r}|)\frac{1}{|\mathbf{p}-\mathbf{r}|^2}\,\mathrm{d}V(\mathbf{r})+\int_{V'_\delta}\exp(-\beta|\mathbf{p}-\mathbf{r}|)\frac{1}{|\mathbf{p}-\mathbf{r}|^2}\,\mathrm{d}V(\mathbf{r}).
\end{aligned} \tag{3.20}$$

For the first integral on the right-hand side of (3.20),

$$\begin{aligned}\int_{B(\mathbf{p};\delta)} \exp(-\beta|\mathbf{p}-\mathbf{r}|)\frac{1}{|\mathbf{p}-\mathbf{r}|^2}\,\mathrm{d}V(\mathbf{r}) &= \int_{B(\mathbf{0};\delta)} \exp(-\beta|\mathbf{r}|)\frac{1}{|\mathbf{r}|^2}\,\mathrm{d}V(\mathbf{r})\\ &= \int_0^\delta \left(\int_{\partial B(\mathbf{0};r)} \exp(-\beta|\mathbf{r}|)\frac{1}{|\mathbf{r}|^2}\,\mathrm{d}S\right)\mathrm{d}r\\ &= 4\pi\int_0^\delta \exp(-\beta r)\,\mathrm{d}r = \frac{4\pi}{\beta}(1-\exp(-\beta\delta)).\end{aligned}$$

Thus the following conclusion holds:

$$\lim_{\delta\to 0}\int_{B(\mathbf{p};\delta)} \exp(-\beta|\mathbf{p}-\mathbf{r}|)\frac{1}{|\mathbf{p}-\mathbf{r}|^2}\,\mathrm{d}V(\mathbf{r}) = 0. \tag{3.21}$$

For the second integral on the right-hand side of (3.20),

$$\begin{aligned}\int_{V'_\delta} \frac{\exp(-\beta|\mathbf{p}-\mathbf{r}|)}{|\mathbf{p}-\mathbf{r}|^2}\,\mathrm{d}V(\mathbf{r}) &\leqslant \int_{B(\mathbf{p};d)\setminus B(\mathbf{p};\delta)} \frac{\exp(-\beta|\mathbf{p}-\mathbf{r}|)}{|\mathbf{p}-\mathbf{r}|^2}\,\mathrm{d}V(\mathbf{r})\\ &= \int_{B(\mathbf{0};d)\setminus B(\mathbf{0};\delta)} \exp(-\beta|\mathbf{r}|)\frac{1}{|\mathbf{r}|^2}\,\mathrm{d}V(\mathbf{r})\\ &= \int_\delta^d \left(\int_{\partial B(\mathbf{0};r)} \exp(-\beta|\mathbf{r}|)\frac{1}{|\mathbf{r}|^2}\,\mathrm{d}S\right)\mathrm{d}r\\ &= 4\pi\int_\delta^d \exp(-\beta r)\,\mathrm{d}r\\ &= \frac{4\pi}{\beta}(\exp(-\beta\delta)-\exp(-\beta d)).\end{aligned}$$

Hence,

$$\lim_{\delta\to 0}\int_{V'_\delta} \exp(-\beta|\mathbf{p}-\mathbf{r}|)\frac{1}{|\mathbf{p}-\mathbf{r}|^2}\,\mathrm{d}V(\mathbf{r}) \leqslant \frac{4\pi}{\beta}(1-\exp(-\beta d)). \tag{3.22}$$

Making use of equations (3.19)–(3.22), one obtains

$$\int_V \exp(-\beta|\mathbf{p}-\mathbf{r}|)\frac{1}{|\mathbf{p}-\mathbf{r}|^2}\chi(\mathbf{p},\mathbf{r})\,\mathrm{d}V(\mathbf{r}) \leqslant \frac{4\pi}{\beta}(1-\exp(-\beta d)).$$

Thus the inequality (3.17) holds.

For the second inequality (3.18), a similar idea is adopted. First, we have

$$\begin{aligned}\int_S \frac{\cos\phi_r}{|\mathbf{p}-\mathbf{r}|^2}\chi(\mathbf{p},\mathbf{r})\,\mathrm{d}S(\mathbf{r}) &= \int_{S'} \frac{\cos\phi_r}{|\mathbf{p}-\mathbf{r}|^2}\,\mathrm{d}S(\mathbf{r})\\ &= \int_{S'_\delta} \frac{(\mathbf{r}-\mathbf{p})\cdot\mathbf{n}_r}{|\mathbf{r}-\mathbf{p}|^3}\,\mathrm{d}S(\mathbf{r}) + \int_{\partial B(\mathbf{p},\delta)} \frac{(\mathbf{r}-\mathbf{p})\cdot\mathbf{n}_r}{|\mathbf{r}-\mathbf{p}|^3}\,\mathrm{d}S(\mathbf{r}).\end{aligned} \tag{3.23}$$

Making use of the divergence theorem, one obtains

$$\int_{S'_\delta} \frac{(\mathbf{r}-\mathbf{p})\cdot\mathbf{n}_r}{|\mathbf{r}-\mathbf{p}|^3}\,\mathrm{d}S(\mathbf{r}) = -\int_{V'_\delta} \nabla\cdot\Big(\frac{\mathbf{r}-\mathbf{p}}{|\mathbf{r}-\mathbf{p}|^3}\Big)\,\mathrm{d}V(\mathbf{r}).$$

And the following result is obvious

$$\nabla\cdot\Big(\frac{\mathbf{r}-\mathbf{p}}{|\mathbf{r}-\mathbf{p}|^3}\Big) = 0 \quad \text{for } \mathbf{r}\in V'_\delta.$$

Therefore,

$$\int_{S'_\delta} \frac{(\mathbf{r}-\mathbf{p})\cdot\mathbf{n}_r}{|\mathbf{r}-\mathbf{p}|^3}\,\mathrm{d}S(\mathbf{r}) = 0. \tag{3.24}$$

For any $\mathbf{r}\in\partial B(\mathbf{p},\delta)$, we have

$$\mathbf{n}_r = \frac{\mathbf{r}-\mathbf{p}}{|\mathbf{r}-\mathbf{p}|}, \quad \mathbf{n}_r\cdot\frac{\mathbf{r}-\mathbf{p}}{|\mathbf{r}-\mathbf{p}|} = 1.$$

Hence,

$$\int_{\partial B(\mathbf{p},\delta)} \frac{(\mathbf{r}-\mathbf{p})\cdot\mathbf{n}_r}{|\mathbf{r}-\mathbf{p}|^3}\,\mathrm{d}S(\mathbf{r}) = \int_{\partial B(\mathbf{p},\delta)} \frac{1}{|\mathbf{r}-\mathbf{p}|^2}\,\mathrm{d}S(\mathbf{r}) = \frac{1}{\delta^2}\int_{\partial B(\mathbf{p},\delta)} 1\,\mathrm{d}S(\mathbf{r}).$$

A simple calculation shows that

$$\int_{\partial B(\mathbf{p},\delta)} \frac{(\mathbf{r}-\mathbf{p})\cdot\mathbf{n}_r}{|\mathbf{r}-\mathbf{p}|^3}\,\mathrm{d}S(\mathbf{r}) = 4\pi. \tag{3.25}$$

Making use of equations (3.23)–(3.25), one obtains

$$\int_S \frac{\cos\phi_r}{|\mathbf{r}-\mathbf{p}|^2}\chi(\mathbf{p},\mathbf{r})\,\mathrm{d}S(\mathbf{r}) = 4\pi.$$

Hence,

$$\int_S \exp(-\beta|\mathbf{p}-\mathbf{r}|)\frac{\cos\phi_r}{|\mathbf{p}-\mathbf{r}|^2}\chi(\mathbf{p},\mathbf{r})\,\mathrm{d}S(\mathbf{r}) \leqslant 4\pi.$$

The proofs are complete. □

With the aid of Lemmas 3.2 and 3.3, some important conclusions are summarized in the following corollary.

**Corollary 3.1.** *The operators $K_1, K_2, K_3, K_4$ are non-negative, and*

$$\|K_1\|_{L^p(S)} < 1-\varepsilon, \quad \|K_2\|_{L^p(S)} < \frac{\varepsilon\sigma_s}{4\beta},$$

$$\|K_3\|_{L^p(V)} < \frac{\sigma_s}{\beta}(1-\exp(-\beta d)), \quad \|K_4\|_{L^p(V)} < \frac{4(1-\varepsilon)}{\varepsilon},$$

*for $p\in[1,\infty]$.*

P r o o f. Let

$$k_1(\mathbf{p},\mathbf{r}) = \frac{1-\varepsilon}{\pi}\exp(-\beta|\mathbf{p}-\mathbf{r}|)\frac{\cos\phi_p\cos\phi_r}{|\mathbf{p}-\mathbf{r}|^2}\chi(\mathbf{p},\mathbf{r}).$$

Let $1 < p < \infty$ and $u \in L^p(S)$. Referring to [28], the following conclusion holds:

$$\begin{aligned}|K_1u(\mathbf{p})| &= \left|\int_S k_1^{1/p+1/q}(\mathbf{p},\mathbf{r})u(\mathbf{r})\,\mathrm{d}S(\mathbf{r})\right| \\ &\leqslant \left(\int_S k_1(\mathbf{p},\mathbf{r})\,\mathrm{d}S(\mathbf{r})\right)^{1/q}\left(\int_S k_1(\mathbf{p},\mathbf{r})|u(\mathbf{r})|^p\,\mathrm{d}S(\mathbf{r})\right)^{1/p}.\end{aligned}$$

Using the inequality (3.11) in Lemma 3.2, we have

$$\begin{aligned}\int_S |K_1u(\mathbf{p})|^p\,\mathrm{d}S(\mathbf{p}) &\leqslant (1-\varepsilon)^{p/q}\int_S\int_S k_1(\mathbf{p},\mathbf{r})|u(\mathbf{r})|^p\,\mathrm{d}S(\mathbf{r})\,\mathrm{d}S(\mathbf{p}) \\ &= (1-\varepsilon)^{p/q}\int_S |u(\mathbf{r})|^p\int_S k_1(\mathbf{p},\mathbf{r})\,\mathrm{d}S(\mathbf{p})\,\mathrm{d}S(\mathbf{r}) \\ &= (1-\varepsilon)^{1+p/q}\int_S |u(\mathbf{r})|^p\,\mathrm{d}S(\mathbf{r}).\end{aligned}$$

Hence,

$$\|K_1\|_{L^p(S)} = \sup_{\|u\|_{L^p(S)}=1}\|K_1u\|_{L^p(S)} \leqslant 1-\varepsilon.$$

The cases with $p = 1$ and $p = \infty$ are straightforward.

Similarly, the other three inequalities can also be proved. □

For practical physical problem, the material parameters satisfy

$$0 < \varepsilon < 1, \quad \beta > 0.$$

Then, we always have

$$\|K_1\|_{L^p(S)} < 1, \quad \|K_3\|_{L^p(V)} < 1. \tag{3.26}$$

With the help of the conclusions in Corollary 3.1, we are now in a position to prove the existence and uniqueness of solution to (2.3).

**Theorem 3.1.** *Let us assume that there exists a constant $0 < \varepsilon_0 < 1$ such that $0 < \varepsilon_0 \leqslant \varepsilon \leqslant 1$. If $\sigma_s/(\beta+\sigma_s) < \varepsilon_0$, then (2.3) has unique solution.*

P r o o f. The unique solvability of (2.3) is equivalent to the reversibility of operator matrix

$$K = \begin{pmatrix} I - K_1 & -K_2 \\ -K_4 & I - K_3 \end{pmatrix}.$$

Using the inequalities (3.26) and the Neumann series theorem, the operators $I-K_1$ and $I - K_3$ are invertible on $L^p(S), L^p(V)$ respectively. Then we have

$$\begin{pmatrix} I & 0 \\ K_4(I-K_1)^{-1} & I \end{pmatrix} K = \begin{pmatrix} I - K_1 & -K_2 \\ 0 & (I-K_3)(I-(I-K_3)^{-1}K_4(I-K_1)^{-1}K_2) \end{pmatrix}.$$

Now, we only need to prove the reversibility of the operator $I - (I - K_3)^{-1}K_4 \times (I - K_1)^{-1}K_2$.

Adopting the Neumann series theorem, we have

$$\|(I-K_1)^{-1}\|_{L^p(S)} \leqslant \frac{1}{1-\|K_1\|_{L^p(S)}}, \quad \|(I-K_3)^{-1}\|_{L^p(V)} \leqslant \frac{1}{1-\|K_3\|_{L^p(V)}}.$$

Then

$$\begin{aligned} \|(I-K_3)^{-1}K_4(I-K_1)^{-1}K_2\|_{L^p(V)} &\leqslant \frac{\|K_2\|_{L^p(S)}\|K_4\|_{L^p(V)}}{(1-\|K_1\|_{L^p(S)})(1-\|K_3\|_{L^p(V)})} \\ &\leqslant \frac{1-\varepsilon}{\varepsilon}\frac{\sigma_s}{\sigma_a+\sigma_s\exp(-\beta d)} \\ &\leqslant \frac{1-\varepsilon_0}{\varepsilon_0}\frac{\sigma_s}{\sigma_a+\sigma_s\exp(-\beta d)}. \end{aligned}$$

According to the Neumann series theorem, the operator $I - (I - K_3)^{-1}K_2 \times (I - K_1)^{-1}K_4$ is reversibility if $\|(I - K_3)^{-1}K_2(I - K_1)^{-1}K_4\|_{L^p(V)} < 1$, that is,

$$\frac{1-\varepsilon_0}{\varepsilon_0}\frac{\sigma_s}{\sigma_a+\sigma_s\exp(-\beta d)} < 1.$$

This equality is equivalent to

$$\frac{1-\varepsilon_0}{\varepsilon_0} < \frac{\sigma_a}{\sigma_s} + \exp(-\beta d).$$

Further, we have

$$\frac{\sigma_a}{\sigma_s} + \exp(-\beta d) < \frac{\sigma_a}{\sigma_s} + 1 = \frac{\beta}{\sigma_s}.$$

So, if

$$\frac{\sigma_s}{\beta+\sigma_s} < \varepsilon_0$$

holds, the reversibility of the operator $I-(I-K_3)^{-1}K_2(I-K_1)^{-1}K_4$ is obtained. The reversibility of the operator matrix

$$\begin{pmatrix} I & 0 \\ K_4(I-K_1)^{-1} & I \end{pmatrix}$$

is obvious.

To sum up, we obtain that

$$K=\begin{pmatrix} I-K_1 & -K_2 \\ -K_4 & I-K_3 \end{pmatrix}.$$

is invertible. □

We note that the assumptions in Theorem 3.1 are satisfied in most situations. First, Theorem 3.1 is valid for radiative heat transfer within black-body boundary of pure absorbing-emitting media. Besides, when the scattering coefficient is small enough, Theorem 3.1 is suitable for any situations with diffuse and gray boundary. For the situation with black boundary, the solvability of the RITEs in any semitransparent media is guaranteed by Theorem 3.1.

## 4. Convergence analysis of an iteration scheme

In order to simulate the coupled integral system (2.3), which is involved in the radiative heat flux and the incident radiation, an iteration scheme is constructed as

$$\begin{cases} q^{(n)}-K_1q^{(n)}=K_2G^{(n)}+f, \\ \qquad G^{(n+1)}=K_3G^{(n)}+K_4q^{(n)}+g, \end{cases} \tag{4.1}$$

where the superscript denotes the number of iteration.

For the iteration scheme (4.1), the following convergence conclusion holds.

**Theorem 4.1.** *Under the hypotheses in Theorem* 3.1, *the iteration scheme* (4.1) *is convergent.*

Proof. We first solve the first equation in (4.1), and the solution is given by

$$q^{(n)}=(I-K_1)^{-1}K_2G^{(n)}+(I-K_1)^{-1}f, \tag{4.2}$$

where we take advantage of the invertibility of the operator $I-K_1$.

Substituting equation (4.2) into the second equation in (4.1), we have

$$G^{(n+1)}=K_3G^{(n)}+K_4((I-K_1)^{-1}K_2G^{(n)}+(I-K_1)^{-1}f)+g. \tag{4.3}$$

Rearranging the right-hand side of (4.3), we have

$$G^{(n+1)} = (K_3 + K_4(I - K_1)^{-1}K_2)G^{(n)} + \tilde{g}, \tag{4.4}$$

where $\tilde{g} = K_4(I - K_1)^{-1}f + g$.

For (4.4), the corresponding error equation can be obtained as

$$e^{(n+1)} = (K_3 + K_4(I - K_1)^{-1}K_2)e^{(n)}, \tag{4.5}$$

where $e^{(n+1)} = G^{(n+1)} - G$.

According to (4.5), it is obvious that the convergence of the iteration scheme (4.1) is equivalent to the contractibility of the operator $K_3 + K_4(I - K_1)^{-1}K_2$:

$$\begin{aligned}\|K_3 + K_4(I - K_1)^{-1}K_2\|_{L^p(V)} &\leqslant \|K_3\|_{L^p(V)} + \|K_4(I - K_1)^{-1}K_2\|_{L^p(V)} \\ &\leqslant \frac{\sigma_s}{\beta}(1 - \exp(-\beta d)) + \frac{\sigma_s}{\beta}\frac{1-\varepsilon}{\varepsilon} \\ &= \frac{\sigma_s}{\beta}\Big(\frac{1}{\varepsilon} - \frac{1}{\exp(\beta d)}\Big) < \frac{\sigma_s}{\beta}\frac{1-\varepsilon_0}{\varepsilon_0}.\end{aligned}$$

According to the assumption, we have

$$\|K_3 + K_4(I - K_1)^{-1}K_2\|_{L^p(V)} < 1. \tag{4.6}$$

The inequality (4.6) implies that the iteration scheme (4.1) is convergent. □

Theorem 4.1 shows that the iteration scheme (4.1) is convergent under the assumptions of Theorem 3.1.

## 5. Numerical discretization and implementation

**5.1. Discretization.** BEM, as a discrete method of a boundary integral equation, is the proper tool to deal with RITEs. In this paper, BEM based on the collocation scheme is used to discretize RITEs.

An alternative integral formula of RITEs can be obtained upon substituting the geometric relationship (3.16) into equations (2.1)–(2.2). The results can be written

as

$$
\begin{aligned}
(5.1)\qquad & q(\mathbf{p}) + \varepsilon E_b(\mathbf{p}) \\
&= \varepsilon \int_S \left( E_b(\mathbf{r}) + \frac{1-\varepsilon}{\varepsilon} q(\mathbf{r}) \right) P_1(\mathbf{p},\mathbf{r})\,\mathrm{d}S(\mathbf{r}) \\
&\quad + \varepsilon \int_S \left( \int_{L_{rp}} I_b(\mathbf{r}') \exp(-\beta|\mathbf{p}-\mathbf{r}'|)\,\mathrm{d}L_{rp}(\mathbf{r}') \right) P_2(\mathbf{p},\mathbf{r})\,\mathrm{d}S(\mathbf{r}) \\
&\quad + \varepsilon \int_S \left( \int_{L_{rp}} G(\mathbf{r}') \exp(-\beta|\mathbf{p}-\mathbf{r}'|)\,\mathrm{d}L_{rp}(\mathbf{r}') \right) P_3(\mathbf{p},\mathbf{r})\,\mathrm{d}S(\mathbf{r}), \quad \mathbf{p} \in S, \\
(5.2)\qquad & G(\mathbf{p}) = \int_S \left( E_b(\mathbf{r}) + \frac{1-\varepsilon_r}{\varepsilon_r} q(\mathbf{r}) \right) P_4(\mathbf{p},\mathbf{r})\,\mathrm{d}S(\mathbf{r}) \\
&\quad + \int_S \left( \int_{L_{rp}} I_b(\mathbf{r}') \exp(-\beta|\mathbf{p}-\mathbf{r}'|)\,\mathrm{d}L_{rp}(\mathbf{r}') \right) P_5(\mathbf{p},\mathbf{r})\,\mathrm{d}S(\mathbf{r}) \\
&\quad + \int_S \left( \int_{L_{rp}} G(\mathbf{r}') \exp(-\beta|\mathbf{p}-\mathbf{r}'|)\,\mathrm{d}L_{rp}(\mathbf{r}') \right) P_6(\mathbf{p},\mathbf{r})\,\mathrm{d}S(\mathbf{r}), \quad \mathbf{p} \in V,
\end{aligned}
$$

where the kernel functions are defined as

$$
\begin{aligned}
P_1(\mathbf{p},\mathbf{r}) &= \exp(-\beta|\mathbf{p}-\mathbf{r}|) \frac{\cos\phi_p \cos\phi_r}{\pi|\mathbf{p}-\mathbf{r}|^2} \chi(\mathbf{p},\mathbf{r}), \\
P_2(\mathbf{p},\mathbf{r}) &= \sigma_a \frac{\cos\phi_p \cos\phi_r}{|\mathbf{p}-\mathbf{r}|^2} \chi(\mathbf{p},\mathbf{r}), \\
P_3(\mathbf{p},\mathbf{r}) &= \frac{\sigma_s}{4\pi} \frac{\cos\phi_p \cos\phi_r}{|\mathbf{p}-\mathbf{r}|^2} \chi(\mathbf{p},\mathbf{r}), \\
P_4(\mathbf{p},\mathbf{r}) &= \exp(-\beta|\mathbf{p}-\mathbf{r}|) \frac{\cos\phi_r}{\pi|\mathbf{p}-\mathbf{r}|^2} \chi(\mathbf{p},\mathbf{r}), \\
P_5(\mathbf{p},\mathbf{r}) &= \sigma_a \frac{\cos\phi_r}{|\mathbf{p}-\mathbf{r}|^2} \chi(\mathbf{p},\mathbf{r}), \\
P_6(\mathbf{p},\mathbf{r}) &= \frac{\sigma_s}{4\pi} \frac{\cos\phi_r}{|\mathbf{p}-\mathbf{r}|^2} \chi(\mathbf{p},\mathbf{r}).
\end{aligned}
$$

To solve equations (5.1)–(5.2) numerically, we use the standard boundary element discretization method [7] in this paper. The boundary of the computational domain is discretized to a set of plane elements denoted by $\{S_k\}_{k=1}^{N_e}$. And $q$ is approximated by linear interpolation on each element. For example, on an element $S_k$, we have

$$
q(\mathbf{p}) = q(\xi,\eta) = \sum_{\alpha=1}^{M} F_\alpha(\xi,\eta) q^\alpha,
$$

where $\xi$, $\eta$ are the intrinsic coordinates, and $F_\alpha(\xi,\eta)$, $q^\alpha$ denote the bilinear shape function and the value of $q$ at a local node $\alpha$ on the element $S_k$. Denote by $M$ the number of nodes on each element.

Let $\mathbf{p}$ in (5.1) be given (in turn) by $\mathbf{p}_i$ for $i = 1, \ldots, N_p$ (where $N_p$ is the number of collocation points on the boundary). Let $\mathbf{p}$ in (5.2) be given (in turn) by $\mathbf{p}_j$ for $j = 1, \ldots, N_i$ (where $N_i$ is the number of collocation points in the interior of the domain). Then equations (5.1)–(5.2) can be approximately written as

$$q_i - \sum_{k=1}^{Ne} \sum_{\alpha=1}^{M} g_{ik}^{\alpha} q^{\alpha} = \sum_{k=1}^{Ne} \sum_{l=1}^{L} f_{ik}^{l} S^{l} + h_i, \quad i = 1, 2, \ldots, N_p, \tag{5.3}$$

$$G_j = \sum_{k=1}^{Ne} \sum_{l=1}^{L} u_{jk}^{l} G^{l} + \sum_{k=1}^{Ne} \sum_{\alpha=1}^{M} v_{jk}^{\alpha} q^{\alpha} + t_j, \quad j = 1, 2, \ldots, N_i, \tag{5.4}$$

where $q_i$, $G_j$ are the abbreviations of $q(\mathbf{p}_i), G(\mathbf{p}_j)$ and

$$\begin{aligned}
g_{ik}^{\alpha} &= (1-\varepsilon) \int_{S_k} F_{\alpha} P_1(\mathbf{p}_i, \mathbf{r}) \, \mathrm{d}S(r), \\
f_{ik}^{l} &= \varepsilon \int_{S_k} \left( \int_{L_{rp}^{l}} \exp(-\beta |\mathbf{p}_i - \mathbf{r}'|) \, \mathrm{d}L(\mathbf{r}') \right) P_3(\mathbf{p}_i, \mathbf{r}) \, \mathrm{d}S(\mathbf{r}), \\
h_i &= \varepsilon \sum_{k=1}^{Ne} \int_{S_k} \sum_{\alpha=1}^{M} F_{\alpha} E_b^{\alpha}(\mathbf{r}) P_1(\mathbf{p}_i, \mathbf{r}) \, \mathrm{d}S(\mathbf{r}) - \varepsilon E_b(\mathbf{p}_i) \\
&\quad + \varepsilon \sum_{k=1}^{Ne} \int_{S_k} \sum_{l=1}^{L} \left( \int_{L_{rp}^{l}} I_b(\mathbf{r}') \exp(-\beta |\mathbf{p}_i - \mathbf{r}'|) \, \mathrm{d}L(\mathbf{r}') \right) P_2(\mathbf{p}, \mathbf{r}) \, \mathrm{d}S(\mathbf{r}), \\
u_{jk}^{l} &= \int_{S_k} \left( \int_{L_{rp}^{l}} \exp(-\beta |\mathbf{p}_j - \mathbf{r}'|) \, \mathrm{d}L(\mathbf{r}') \right) P_6(\mathbf{p}_j, \mathbf{r}) \, \mathrm{d}S(\mathbf{r}), \\
v_{jk}^{\alpha} &= \frac{1-\varepsilon}{\varepsilon} \int_{S_k} F_{\alpha} P_4(\mathbf{p}_j, \mathbf{r}) \, \mathrm{d}S(\mathbf{r}), \\
t_j &= \sum_{k=1}^{Ne} \int_{S_k} \sum_{\alpha=1}^{M} F_{\alpha} E_b^{\alpha}(\mathbf{r}) P_4(\mathbf{p}, \mathbf{r}) \, \mathrm{d}S(\mathbf{r}) \\
&\quad + \sum_{k=1}^{Ne} \int_{S_k} \sum_{l=1}^{L} \left( \int_{L_{rp}^{l}} I_b(\mathbf{r}') \exp(-\beta |\mathbf{p}_j - \mathbf{r}'|) \, \mathrm{d}L(\mathbf{r}') \right) P_5(\mathbf{p}_j, \mathbf{r}) \, \mathrm{d}S(\mathbf{r}),
\end{aligned}$$

where $\{L_{rp}^{l}\}_{l=1}^{L}$ denotes the subdivision of the line $L_{rp}$.

Then system (5.3)–(5.4) is solved by the iteration scheme (4.1).

The computational domain is covered by the regular grid of cuboid cells in order to calculate the line integral. When the temperature and incident radiation within each small cuboid cell are assumed to be constants, the line integrals in $f_{ik}^{l}$, $h_i$, $u_{jk}^{l}$, $t_j$ can be calculated analytically. The nearly singular term, $1/|\mathbf{p} - \mathbf{r}|^2$, can be handled by the technique proposed by Eberwien et al. [13]. The idea in [13] allows us to ensure that the error introduced by numerical integration is nearly constant, regardless of

the proximity of the source point. The detailed procedure is not repeated here. We refer the interested readers to [13].

Note that the Boolean function in integral kernels needs to be determined by an effective visualization algorithm. This procedure is very time-consuming. In addition, the accurate detection of the shadow regions is an arduous and crucial task and affects greatly the accuracy of the numerical simulation. The aim of the next subsection is to develop a high-precision visualization algorithm.

**5.2. The algorithm for the shadow detection.** For the three dimensional problem, the present algorithm is valid for the plane elements. Due to the prohibitively long computing time, the discretization strategy with non-plane elements is not applied to the calculation of thermal radiation.

First, some symbols need to be explained. The quantity $\mathbf{p}$ denotes the source point. The unit outward normal vector at $\mathbf{p}$ will be denoted by $\mathbf{n}_p$. The symbols $S_k$ and $S_b$ represent the current element on which the integration may be performed and the third party element which may prevent the radiation ray from reaching its destination, respectively. Let $\mathbf{n}_k$ denote the unit outward normal vector of the plane element $S_k$. Let $\mathbf{r}$, $\mathbf{r}_i$ $(i = 1, 2, 3, \ldots)$ denote the centre point and vertices of $S_k$.

The key step in the present algorithm is to create two lists. One is the list of active elements, from which the radiation energy is emitted to the destination point $\mathbf{p}$. The other is the list of blocking elements, in which the element prevents the radiation ray from reaching its designated destination. Finally, for the active element, which can be seen totally, the integration is carried out directly, while the active element, which is shaded partially, needs to be subdivided. The element, which is shaded totally, is discarded.

Now the detailed detection-subdivision procedure is described as follows:

*Step 1.* Creation of the list of active elements.

This list is built as the procedure proceeds.

Let

$$d_1 = \mathbf{n}_p \cdot (\mathbf{p} - \mathbf{r}), \quad d_2 = \mathbf{n}_k \cdot (\mathbf{r} - \mathbf{p}).$$

If the signs of $d_1$, $d_2$ are both positive, the current element $S_k$ is viewed as an active element and it is added to the list of active elements. Repeating this operation for all boundary elements, we have created the initial list of active elements for $\mathbf{p}$.

*Step 2.* Creation of the list of blocking elements.

For any potential active element, the list of blocking elements is established by scanning all other elements by the following operations.

First, the potential active elements which are coplanar with $\mathbf{p}$, are excluded. For the other elements, a cylinder window is created as in Figure 1, of which the diameter

is the sum of diameters of the potential active element and the potential blocking element, and the height is $|\mathbf{p} - \mathbf{r}|$.

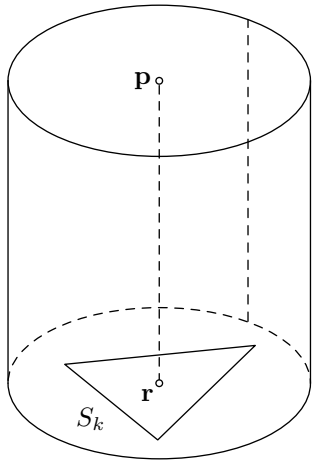


Figure 1. The cylinder window for point $\mathbf{p}$ and the potential active element $S_k$.

A potential blocking element $S_b$, if its center lies outside of this cylinder, is discarded and then the next element is considered. If the center of $S_b$ lies in this cylinder, the following operations are performed on this element.

A cone window is constructed as in Figure 2. The bottom diameter of the cone is equal to the diameter of $S_k$ and its height is $|\mathbf{p} - \mathbf{r}|$. If one of the vertices of $S_b$ lies in this cone, $S_b$ is put into the list of blocking elements about $\mathbf{p}$ and $S_k$. Otherwise, more operations are needed to exclude the situation as shown in Figure 3.

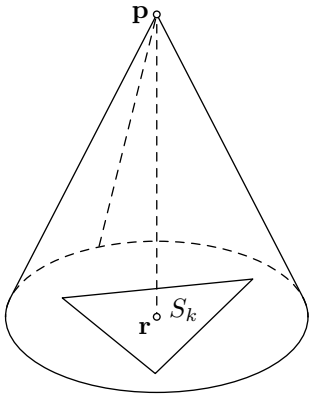


Figure 2. The cone window for point $\mathbf{p}$ and the potential active element $S_k$.

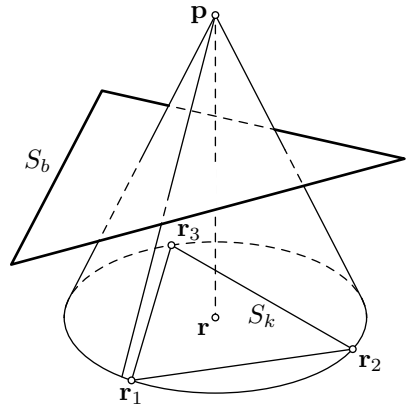


Figure 3. The sight from $\mathbf{p}$ to $S_k$ is shaded totally.

The line segment **pr** is constructed. If **pr** intersects with $S_b$, we can conclude that $S_k$ cannot be viewed from **p**. The element $S_k$ is discarded from the initial list of active elements and then we go back to the beginning of step 2. If **pr** does not intersect with $S_b$, the line segments connecting the source point **p** and the vertices of $S_k$ ($\mathbf{pr}_1, \mathbf{pr}_2, \mathbf{pr}_3, \ldots$) are constructed. If one of these segments intersects with $S_b$, $S_b$ is put into the list of blocking elements. If none of these segments intersects $S_b$, $S_b$ is discarded.

The above operations are repeated for all the boundary elements. Then the list of blocking elements is established for **p** and $S_k$.

A possible case is that $S_k$ may be shaded by the union of some adjacent blocking elements. A further operation is needed in order to check this situation. We first need to determine whether the line segments connecting the source point **p** and the vertices of $S_k$ intersect with some blocking element in the list of blocking elements or not. If the proposition is true for all these segments, $S_k$ is discarded from the list of active elements. Otherwise, no operation is performed.

*Step 3.* Subdivision of the active element.

After the previous steps, a list of active elements for point **p** is established. Meanwhile, a list of blocking elements about any active element is established. For any active element, if its list of blocking elements is empty, the numerical integration is performed directly. For the remaining active elements, a subdivision is performed as follows.

First, this active element is subdivided into four sub-elements as shown in Figure 4.

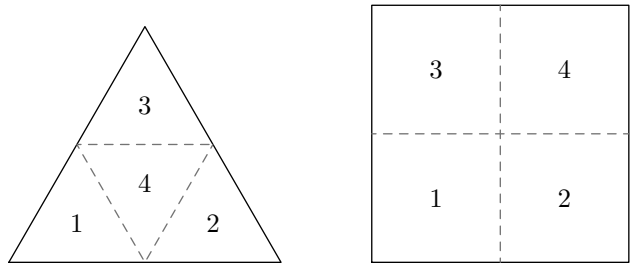


Figure 4. Subdivision of element.

For all the sub-elements, step 2 above is performed throughout its list of blocking elements. When some sub-element is blocked partially, it is subdivided into four smaller sub-elements. For sub-element totally visible, the integration on this sub-element is performed. On the contrary, the sub-element totally shaded is discarded.

The subdivision procedure is terminated when the area of the sub-element reaches a preset minimum value. The accuracy of the present algorithm increases as the

preset minimum value reduces. The preset minimum value can be set to be an arbitrary small quantity. In the following numerical examples, it takes $10^{-4}$.

Although the present algorithm is described based on 3D geometry, it can be applied to 2D geometries naturally. For 2D problems, the two windows in step 2 are rectangle and triangle, respectively.

## 6. Numerical experiments

**6.1. Test 1.** In this subsection, a 3D L-shaped domain is considered (see Figure 5). The dimensions of this tested geometry are $W \times L \times H = 1 \times 3 \times 3$ ($\mathrm{m}^3$). The domain contains an emitting-absorbing medium at a temperature of 1000 K. The walls are black ($\varepsilon = 1$) at 500 K. Figure 6 shows the effect of the absorbing coefficient of the medium on the predicted net radiative heat flux along the $AA$ line.

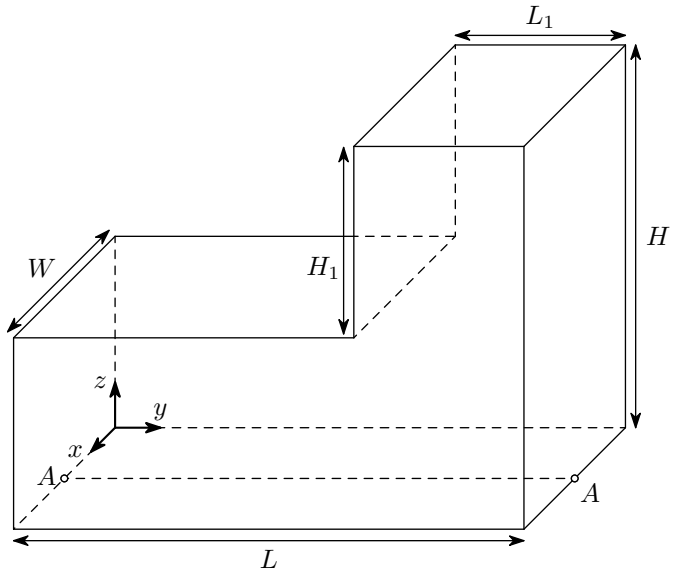


Figure 5. The L-shaped enclosure.

The present model uses 2200 boundary elements. The comparisons with the existing results are shown in Figure 6. From the comparisons, the validity of the present algorithm is verified. The proposed numerical procedure can be viewed as a good alternative technique for the simulation of thermal radiation in complex enclosures.

**6.2. Test 2.** The analysis of radiative transfer of multidimensional rectangular geometries has been associated with the design of combustion chambers and furnaces. For this test we refer to [28]. As shown in Figure 7, a standard unit cube is considered.

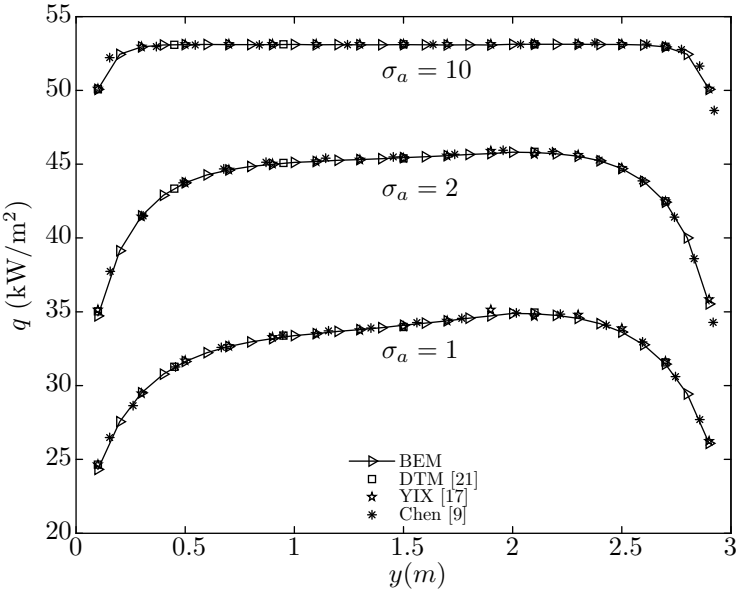


Figure 6. Net radiative heat flux along line $AA$.

All six walls of the cube are black ($\varepsilon = 1$). The scattering albedo of medium is equal to unity ($\Omega = \sigma_s/\beta = 1$). All the walls, as well as the medium in the enclosure, are kept cold ($T = 0\,\mathrm{K}$). Only the emissive power of the bottom wall is taken $1.0\,\mathrm{W/m^2}$.

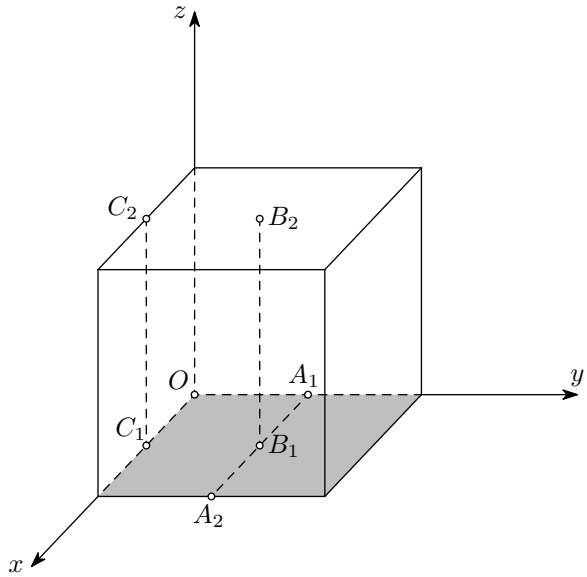


Figure 7. System geometry.

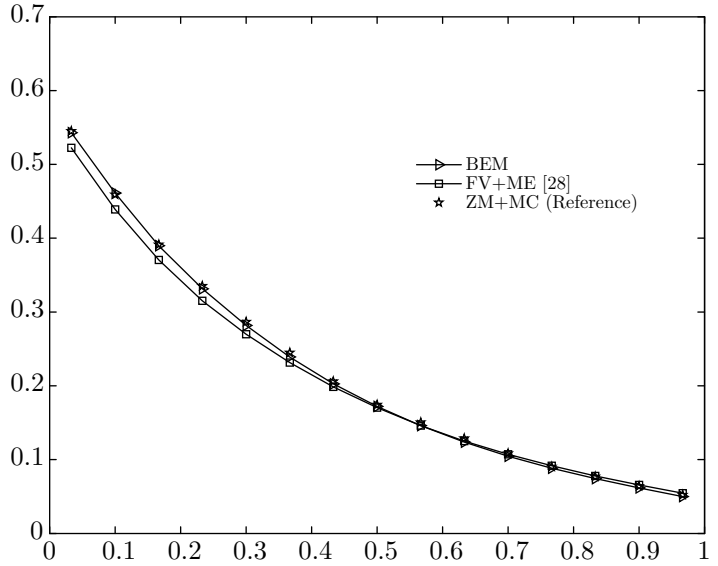


Figure 8. Non-dimensional net radiative heat flux in z-direction along with $C_1C_2$.

As in [28], we also consider the dimensionless heat flux at $A_1A_2$, $C_1C_2$ and the average incident radiation at $B_1B_2$. The numerical comparisons are shown in Figures 8–10. The present model uses 1350 boundary elements and 1331 cuboid cells in the medium. From the comparative results, the present results are similar to the references compared with the FV+ME.

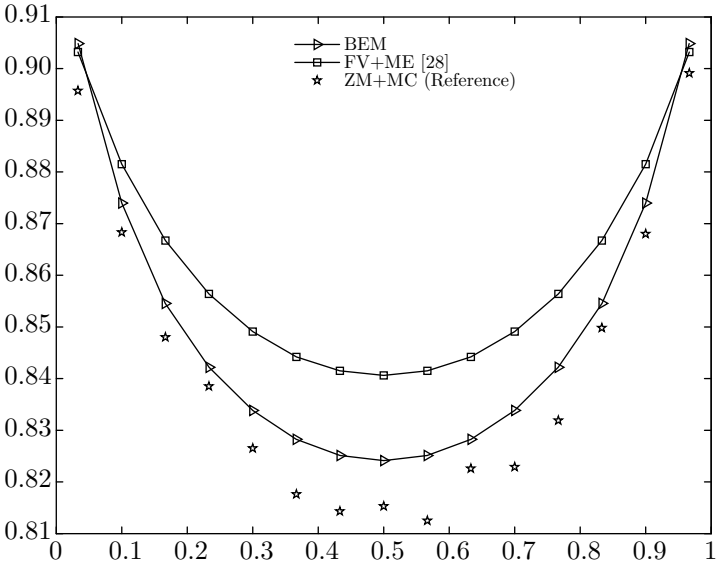


Figure 9. Non-dimensional net radiative heat flux in x-direction along with $A_1A_2$.

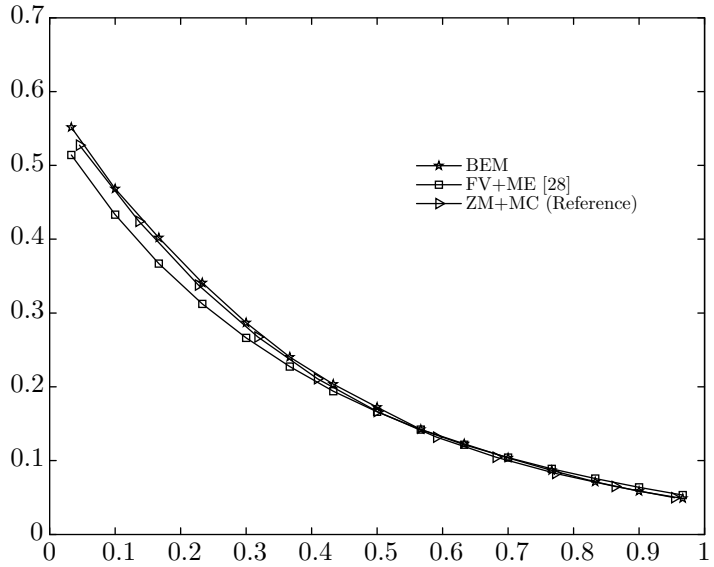


Figure 10. Non-dimensional average incident radiation in z-direction along with $B_1B_2$.

## 7. Conclusions

In this paper we first analyzed the properties of the four integral operators associated with the RITEs model. Those properties allow us to prove the existence and uniqueness of solutions to the RITEs model. We then proposed an iteration algorithm, which serves as a nonlinear solver for our simulation of the RITEs model, and established its convergence. An improved high-precision visibility algorithm was developed to overcome the difficulty caused by geometries of non-convex domains. Finally, we presented two numerical experiments to verify the effectiveness and accuracy of the proposed numerical method and algorithms. Admittedly, the amount of computation involved in the realization of our method and algorithms are still huge for three-dimensional simulations. One of our near term research projects is to improve efficiency of the proposed numerical method and to develop more effective methods and algorithms which are better suited for implementation on high performance computers.

A c k n o w l e d g m e n t s . The authors thank Professor Xiaobing Feng of the University of Tennessee for his valuable suggestions and for his help on improving the presentation of the paper.

*References*


[1] *M. L. Adams, E. W. Larsen*: Fast iterative methods for discrete-ordinates particle transport calculations. Progr. Nucl. Energy *40* (2002), 3–159. doi

[2] *V. Agoshkov*: Boundary Value Problems for Transport Equations. Modeling and Simulation in Science, Engineering and Technology, Birkhäuser, Boston, 1998. zbl MR doi

[3] *Z. Altaç, M. Tekkalmaz*: Benchmark solutions of radiative transfer equation for three-dimensional rectangular homogeneous media. J. Quant. Spect. Rad. Transfer *109* (2008), 587–607. doi

[4] *Z. Altaç, M. Tekkalmaz*: Exact solution of radiative transfer equation for three-dimensional rectangular, linearly scattering medium. J. Thermophys. Heat Transf. *25* (2011), 228–238. doi

[5] *K. Atkinson, G. Chandler*: The collocation method for solving the radiosity equation for unoccluded surfaces. J. Integral Equations Appl. *10* (1998), 253–290. zbl MR doi

[6] *K. Atkinson, D. D.-K. Chien, J. Seol*: Numerical analysis of the radiosity equation using the collocation method. ETNA, Electron. Trans. Numer. Anal. *11* (2000), 94–120. zbl MR

[7] *R. A. Białecki, Ł. Grela*: Application of the boundary element method in radiation. Mech. Teor. Stosow. *36* (1998), 347–364. zbl

[8] *J. Blobner, R. A. Białecki, G. Kuhn*: Boundary-element solution of coupled heat conduction-radiation problems in the presence of shadow zones. Numer. Heat Transfer, Part B *39* (2001), 451–478. doi

[9] *S.-S. Chen, B.-W. Li, X.-Y. Tian*: Chebyshev collocation spectral domain decomposition method for coupled conductive and radiative heat transfer in a 3D L-shaped enclosure. Numer. Heat Transfer, Part B *70* (2016), 215–232. doi

[10] *M. F. Cohen, J. R. Wallace*: Radiosity and Realistic Image Synthesis. Academic Press Professional, Boston, 1993. zbl

[11] *A. L. Crosbie, R. G. Schrenker*: Exact expressions for radiative transfer in a three-dimensioanl rectangular geometry. J. Quant. Spect. Rad. Transfer *28* (1982), 507–526. doi

[12] *A. L. Crosbie, R. G. Schrenker*: Radiative transfer in a two-dimensional rectangular medium exposed to diffuse radiation. J. Quant. Spect. Rad. Transfer *31* (1984), 339–372. doi

[13] *U. Eberwien, C. Duenser, W. Moser*: Efficient calculation of internal results in 2D elasticity BEM. Eng. Anal. Bound. Elem. *29* (2005), 447–453. zbl doi

[14] *A. F. Emery, O. Johansson, M. Lobo, A. Abrous*: A comparative study of methods for computing the diffuse radiation viewfactors for complex structures. J. Heat Transfer *113* (1991), 413–422. doi

[15] *O. Hansen*: The local behavior of the solution of the radiosity equation at the vertices of polyhedral domains in $\mathbb{R}^3$. SIAM J. Math. Anal. *33* (2001), 718–750. zbl MR doi

[16] *J. R. Howell, M. P. Mengüç, R. Siegel*: Thermal Radiation Heat Transfer. CRC Press, Boca Raton, 2010. doi

[17] *P.-F. Hsu, Z. Tan*: Radiative and combined-mode heat transfer within L-shaped nonhomogeneous and nongray participating media. Numer. Heat Transfer, Part A *31* (1997), 819–835. doi

[18] *R. Kress*: Linear Integral Equations. Applied Mathematical Sciences 82, Springer, New York, 2014. zbl MR doi

[19] *M. T. Laitinen, T. Tiihonen*: Integro-differential equation modelling heat transfer in conducting, radiating and semitransparent materials. Math. Methods Appl. Sci. *21* (1998), 375–392. zbl MR doi

[20] *B. Q. Li, X. Cui, S. P. Song*: The Galerkin boundary element solution for thermal radiation problems. Eng. Anal. Bound. Elem. *28* (2004), 881–892. zbl doi

[21] *W. M. Malalasekera, E. H. James*: Radiative heat transfer calculations in three-dimensional complex geometries. ASME J. Heat Transfer *118* (1996), 225–228. doi

[22] *M. F. Modest*: Radiative Heat Transfer. Academic Press, Oxford, 2013. doi
[23] *N. A. Qatanani, A. Daraghmeh*: Asymptotic error analysis for the heat radiation boundary integral equation. Eur. J. Math. Sci. *2* (2013), 51–61.
[24] *B. Sun, D. Zheng, B. Klimpke, B. Yildir*: Modified boundary element method for radiative heat transfer analyses in emitting, absorbing and scattering media. Eng. Anal. Bound. Elem. *21* (1998), 93–104. zbl doi
[25] *Z. Tan*: Radiative heat transfer in multidimensional emitting, absorbing, and anisotropic scattering media: mathematical formulation and numerical method. J. Heat Transfer *111* (1989), 141–147. doi
[26] *S. T. Thynell*: The integral form of the equation of transfer in finite, two-dimensional, cylindrical media. J. Quant. Spect. Rad. Transfer *42* (1989), 117–136. doi
[27] *T. Tiihonen*: Stefan-Boltzmann radiation on non-convex surfaces. Math. Methods Appl. Sci. *20* (1997), 47–57. zbl MR doi
[28] *D. N. Trivic, C. H. Amon*: Modeling the 3-D radiation of anisotropically scattering media by two different numerical methods. Int. J. Heat Mass Transfer *51* (2008), 2711–2732. zbl doi
[29] *R. Viskanta*: Radiation transfer and interaction of convection with radiation heat transfer. Adv. Heat Transfer *3* (1966), 175–251. zbl doi
[30] *A. Watt*: Fundamentals of Three-Dimensional Computer Graphics. Addison-Wesley Publishing Company, Wokingham, 1989. zbl

*Authors' address*: *Yao-Chuang Han*, *Yu-Feng Nie*, *Zhan-Bin Yuan*, Department of Applied Mathematics, Northwestern Polytechnical University, Xian, Shaanxi, China, 710129, e-mail: hychuang2013@mail.nwpu.edu.cn, yfnie@mail.nwpu.edu.cn, yzzzb@nwpu.edu.cn.